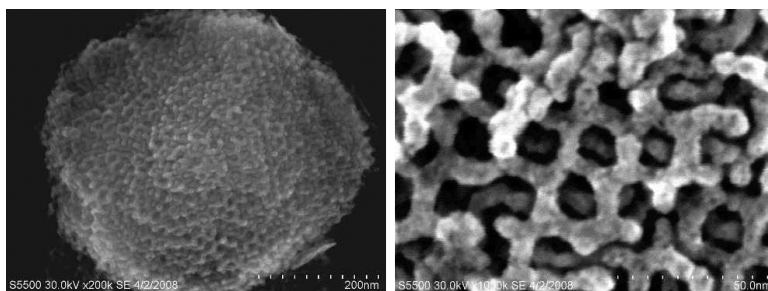Communication

Pseudomorphic Transformation of Highly Ordered Mesoporous CoO to CoO via Reduction with Glycerol

Harun Tu#ysu#z, Yong Liu, Claudia Weidenthaler, and Ferdi Schu#th

More About This Article

Additional resources and features associated with this article are available within the HTML version:

- Supporting Information
- Access to high resolution figures
- Links to articles and content related to this article
- Copyright permission to reproduce figures and/or text from this article

View the Full Text HTML

ACS Publications
High quality. High impact.

Pseudomorphic Transformation of Highly Ordered Mesoporous Co$_3$O$_4$ to CoO via Reduction with Glycerol

Harun Tüysüz, Yong Liu, Claudia Weidenthaler, and Ferdi Schüth*

Max-Planck Institut für Kohlenforschung, Kaiser-Wilhelm-Platz 1, D-45470 Mülheim an der Ruhr, Germany

Received August 14, 2008; E-mail: schueth@mpi-muelheim.mpg.de

Ordered mesoporous materials are interesting because of their special framework topologies, high surface areas, and controllable particle sizes, pore sizes, and pore volumes.[1,2] These properties make the materials interesting in different application areas including catalysis,[3,4] sorption,[5] separation,[6,7] drug delivery,[8,9] sensors,[10] photonics,[11] and magnetism.[12,13] The first templated ordered mesoporous materials were synthesized around 1990 using soft templating pathways.[14,15] Following the soft templating pathway different kinds of ordered mesoporous silicas[16,17] and nonsilica materials such as Cr$_2$O$_3$,[18] γ-Al$_2$O$_3$,[19] TiO$_2$, ZrO$_2$, Al$_2$O$_3$, Nb$_2$O$_5$, Ta$_2$O$_5$, and WO$_3$ were successfully synthesized.[20] Lyons et al. fabricated a series of mesoporous lanthanide oxides using hexadecylamine as a soft template.[21] Nanocasting is an alternative method to prepare materials that are difficult to synthesize by conventional pathways.[22,23] This hard templating approach has been applied to produce different kinds of metal oxides, such as Co$_3$O$_4$,[24−26] Cr$_2$O$_3$,[27,28] Mn$_3$O$_4$,[29] α-Fe$_2$O$_3$,[30] γ-Fe$_2$O$_3$, Fe$_3$O$_4$,[31] 2-line ferrihydrite,[13] and NiO.[32] Lu et al. reported that in principle it is possible to take the nanocasting process one step further and use the nanocast carbon CMK-3 as a matrix for the preparation of ordered mesoporous silica. Although this brings one only back to the starting point, it proved the possibility to use ordered porous carbons to template ordered inorganic materials.[33] Following this work, several ordered mesoporous materials like MgO,[34] boron nitride,[35] γ-Al$_2$O$_3$,[36] aluminosilicate,[37] CuO,[38] and ZnO[39] were nanocast using ordered mesoporous carbon as a hard template.

Cobalt monoxide, CoO, crystallizes in the rock salt structure where Co^{2+} ions are octahedrally coordinated by lattice oxygen. Nanostructured CoO materials have attracted much attention because they exhibit superparamagnetism or weak ferromagnetism and thus have potential applications based on their magnetic properties.[40] Nanostructured CoO materials (nanoparticles or nanocrystalline samples) have mainly been prepared by thermal decomposition of metal-surfactant complexes in high boiling solvents or by controlled oxidation of Co$_2$(CO)$_8$ or metallic cobalt nanoparticles.[41,42] Another possible method to obtain CoO is the reduction of other cobalt oxides such as Co$_3$O$_4$ and Co$_2$O$_3$. Zhang et al. reported the preparation of monodisperse tetrapod-shaped CoO nanocrystals via an alcoholysis route using Co$_2$O$_3$ as precursor and dodecanol as solvent and reducing agent.[43] Alcohols have been used also in other oxide reduction processes. The preparation of metal powders through alcoholysis or the polyol process has mainly been focused on ethylene glycol or diethylene glycol or their mixtures as reducing agents.[44,45] Sinha et. al reported the preparation of silver nanoparticles using glycerol as solvent and reducing agent.[46]

In this report, we describe the exploration of possibilities for a pseudomorphic reduction of ordered mesoporous metal oxides by high temperature treatment with glycerol, which was most thor-
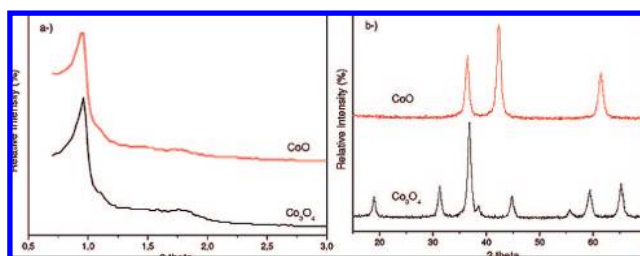

Figure 1. Low (a) and wide (b) angle XRD patterns of the samples before (Co$_3$O$_4$) and after (CoO) glycerol treatment.

oughly studied as an example of the reaction of Co$_3$O$_4$ to CoO. The glycerol process is a gentle reduction procedure, which maintains the framework topology on the mesoscale (thus we use the term pseudomorphic) while changing the oxidation state and the structure at the atomic scale. Such a pseudomorphic reduction of a mesostructured metal oxide had previously only been achieved for the cases of Mn$_3$O$_4$[29] and Fe$_3$O$_4$[31] with hydrogen as reductant.

Mesoporous CoO has not been synthesized either by soft templating or by nanocasting, and it is difficult to prepare by these pathways. Thus, it appeared to be an ideal example for this study by conventional pathways. First, ordered mesoporous Co$_3$O$_4$ was obtained via nanocasting using KIT-6 as a hard template which had been aged at 80 °C. Detailed information on synthesis and characterization of mesoporous Co$_3$O$_4$ is presented elsewhere.[26] Nanocast Co$_3$O$_4$ has a BET surface area of 113 m^2 g^{-1} and a pore volume of 0.184 cm^3 g^{-1} (see Supporting Information Figure S1 for the isotherm and pore size distribution of Co$_3$O$_4$). The reduction of 150 mg of mesostructured Co$_3$O$_4$ was carried out at 320 °C in a fixed bed reactor with a stainless steel inlet (7 mm inner diameter). A glycerol aqueous solution (50 wt %) was pumped into the reactor at a flow rate of 1 mL/h with a syringe pump (Pharmacia Fine Chemicals P-500) and evaporated at the outlet of the capillary. The reduction time was 15 h, and during the process no carrier gas was used. Afterward, the reactor was cooled down to room temperature under a nitrogen flow of 20 mL/h.

The structure of the crystalline phases was examined by X-ray diffraction (XRD). The low and wide angle XRD patterns of Co$_3$O$_4$ before and after glycerol treatment are given in Figure 1. As one can see from the low angle XRD patterns (Figure 1a), after the glycerol treatment the ordered mesostructure is preserved, the low angle pattern is almost unchanged. The (211) and (220) reflections are characteristic for the cubic ordered structure with $Ia\bar{3}d$ symmetry. The unit cell parameter was estimated from the position of the (211) reflection to be 22.9 nm.

Possible reduction products of Co$_3$O$_4$ are CoO, metallic cobalt, or a mixture of both. The crystalline phase present after glycerol treatment is identified by XRD as pure CoO (Figure 1b). Neither
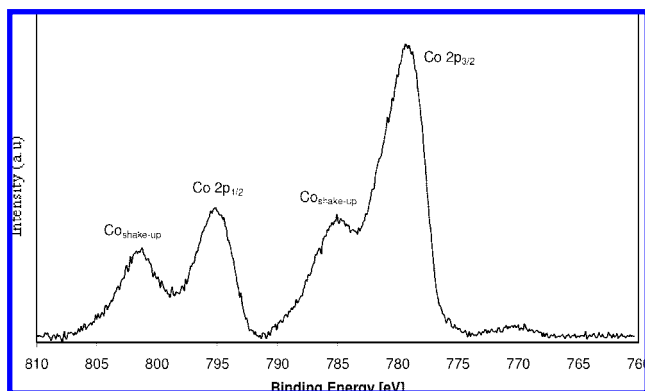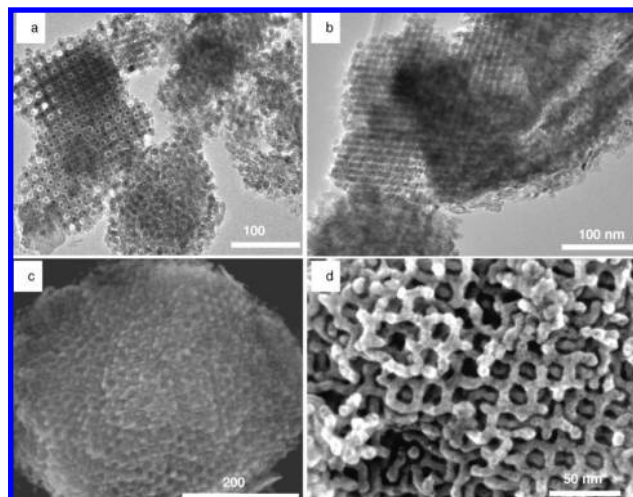
Figure 2. XPS spectrum of Co 2p for cubic ordered mesoporous CoO.
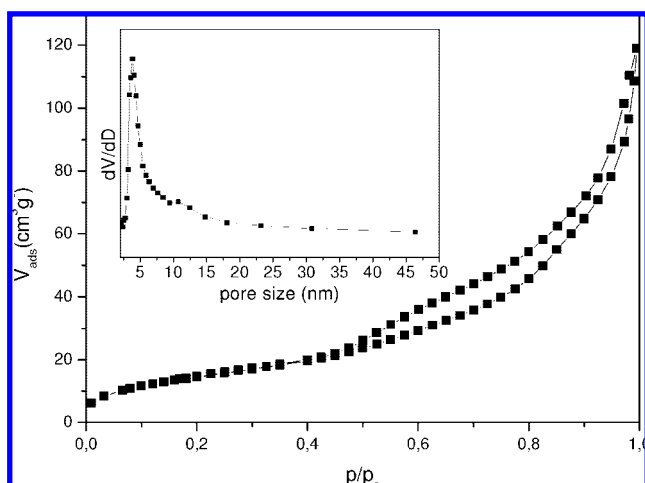
Figure 3. N$_2$-sorption isotherm and pore size distribution (insert) for cubic ordered mesoporous CoO.

Figure 4. TEM images of Co$_3$O$_4$ (a) and CoO (b) and HR-SEM images of cubic ordered mesoporous CoO (c, d).

metallic cobalt nor residual Co$_3$O$_4$ could be observed in the XRD pattern. However, amounts below 1−3 wt % of crystalline compounds cannot be detected by powder diffraction methods. To obtain additional information on the possible presence of metallic cobalt or Co$_3$O$_4$, the samples were also analyzed by X-ray photoelectron spectroscopy (XPS). The narrow scan of the Co 2p binding energy range is shown in Figure 2. For an unambiguous assignment of the binding energy, reference samples were investigated (not shown here). The spin orbit doublet shows satellite peaks (shake-off) typical for the Co^{2+} oxidation state. In agreement with the XRD data, also XPS thus excludes the presence of metallic cobalt at an appreciable concentration level.

The pore structures of mesoporous CoO were examined by N$_2$-sorption measurement; the results are presented in Figure 3. The isotherm is type IV with an H1 hysteresis loop similar to nanocast Co$_3$O$_4$. The material has a BET surface area of 55 m^2/g and a pore volume of 0.138 cm^3/g. The pore size distribution calculated from the desorption isotherm by the BJH method is centered at 4 nm. However, as one can see from the insert in Figure 3, there is also a peak around 12 nm. The KIT-6 silica template has two pore systems. During the preparation of the nanocast Co$_3$O$_4$, the metal oxide can grow in one or both pore systems. If it grows homogenously in both pore systems, a nanocast metal oxide with a uniform pore size distribution would result. If metal oxide partly forms only in one of the enantionmeric pore systems of the template, this leads to a replica with a bimodal pore size distribution.[26,32]

This bimodal size distribution is retained after the pseudomorphic reduction by glycerol.

The structure and morphology of mesoporous CoO were further examined by TEM and HR-SEM (Figure 4). The TEM images of the Co$_3$O$_4$ before and after reduction are presented in Figure 4a and b, respectively. As one can see from Figure 4a, nanocast Co$_3$O$_4$ consists of a coupled and an uncoupled ordered subframework. The well ordered structure of the CoO after the reduction can be seen clearly from the TEM images (Figure 4a). The particle size of the sample is in the range 150−1200 nm, and detailed analysis gives an average crystallite size of ∼8 nm for the individual domains forming the mesostructure, in good agreement with the value obtained from the XRD pattern by the Scherrer equation (10 nm). The Co$_3$O$_4$ domains prior to reduction had a size of 11 nm, suggesting that the individual domains retain their identity during reduction.

HR-SEM images of the sample are in agreement with the N$_2$-sorption measurements. The HR-SEM analysis reveals two types of structures in the materials. Figure 4c shows a coupled, dense framework, while Figure 4d presents mostly an open uncoupled framework structure; both were found in the same sample. As mentioned already, if the metal oxide grows homogenously in both channels of the KIT-6 template, a replica with a coupled subframework and only one pore system could be obtained. If the metal oxide grows (in part of the template silica) within only one of the channel systems of the KIT-6 structure, the resulting nanocast metal oxide will have an uncoupled subframework beside the coupled subframework. In this case the nanocast metal oxide shows a bimodal pore size distribution. As one can see from the HR-SEM images (Figure 4d), in the case of the uncoupled subframework structure CoO has an average pore size of ∼12 nm in good agreement with N$_2$-sorption measurement (Figure 3, insert).

To further explore the novel glycerol reduction pathway, different reducing agents and reaction conditions to optimize the preparation pathway were studied. Longer reduction times, such as 24 h, gave essentially the same results. The reduction of nanocast Co$_3$O$_4$ could not be investigated at much lower temperatures than 320 °C, because condensation of glycerol would occur due to the high partial pressure and the high boiling point of glycerol. If pure H$_2$ is used as the reducing agent (15 h at 320 °C), a mixture of metallic Co, CoO, and Co$_3$O$_4$ is obtained. Additionally, the ordered structure is destroyed. H$_2$ is a very strong reducing agent but not very efficient

for the reduction of Co_3O_4 to CoO. The reduction of Co_3O_4 was also investigated in the liquid phase. Ordered mesoporous Co_3O_4 (150 mg) was refluxed in 10 mL of a glycerol aqueous solution (50 wt %). After 72 h of refluxing, the XRD pattern of the sample indicates the presence of pure Co_3O_4. This confirms that the reduction does not happen in the liquid phase.

To explore the transferability of the method to other compounds, we extended the investigations to iron oxide. Recently, we reported the preparation of ordered mesoporous ferrihydrite via the nanocasting route.[13] Ferrihydrite is a reddish-brown, antiferromagnetic material. After exposure to a flow of glycerol for 15 h at 320 °C, we obtained a black ferromagnetic solid. After glycerol treatment, the reflections in the low angle XRD pattern of the sample have lost some intensity but the presence of an ordered structure is still identifiable. The wide angle XRD pattern shows the presence of the pure crystalline Fe_3O_4 phase (see Supporting Information Figure S2, for low and wide angle XRD patterns). This confirms that the glycerol process can be applied to other metal oxide systems. Further studies related to the reduction of ferrihydrite and other metal oxides are in progress in our laboratory.

In conclusion, we have prepared an ordered mesostructured CoO by the reduction of nanocast Co_3O_4 using glycerol as reducing agent. The structure and morphology of the materials were fully characterized. HR-TEM and HR-SEM reveal a highly ordered structure, and the wide angle XRD pattern indicates a single crystalline phase of CoO. Preliminary results on the glycerol reduction of mesostructured ferrihydrite reveal that the pseudomorphic reduction process is more generally applicable, and it is expected that other low valence state oxides can be synthesized via this method.

Supporting Information Available: N_2-sorption isotherm for nanocast Co_3O_4, low and wide angle XRD patterns of ordered mesoporous ferrihydrite before and after glycerol treatment. This material is available free of charge via Internet at http://pubs.acs.org.

References

(1) Schüth, F. Chem. Mater. 2001, 13, 3184.
(2) Wan, Y.; Zhao, D. Chem. Rev. 2007, 107, 7.
(3) Corma, A. Chem. Rev. 1997, 97, 2373.
(4) Tüysüz, H.; Comotti, M.; Schüth, F. Chem. Commun. 2008, 4022.
(5) Kruk, M.; Jaroniec, M. Chem. Mater. 2001, 13, 3169.
(6) MacLachlan, M. J.; Coombs, N.; Ozin, G. A. Nature 1999, 397, 681.
(7) Martin, T.; Galarneau, A.; Di Renzo, F.; Brunel, D.; Fajula, F.; Heinisch, S.; Cretier, G.; Rocca, J. L. Chem. Mater. 2004, 15, 1725.
(8) Mellaerts, R.; Aerts, C. A.; Van Humbeeck, J.; Augustijns, P.; Van den Mooter, G.; Martens, J. A. Chem. Commun. 2007, 1375.
(9) Yang, P. P.; Quan, Z. W.; Lu, L. L.; Huang, S. S.; Lin, J.; Fu, H. G. Nanotechnology 2007, 18, 235703.
(10) Hyodo, T.; Nishida, N.; Shimizu, Y.; Egashira, M. Sens. Actuators, B 2002, 83, 209.
(11) Fuertes, M. C.; López-Alcaraz, F. J.; Marchi, M. C.; Troiani, H. E.; Luca, V.; Míguez, G.; Soler-Illia, J. A. A. Adv. Funct. Mater. 2007, 17, 1247.
(12) Lu, A. H.; Schmidt, W.; Matoussevitch, N.; Bönnermann, H.; Spliethoff, B.; Tesche, B.; Bill, E.; Kiefer, W.; Schüth, F. Angew. Chem., Int. Ed. 2004, 43, 4303.
(13) Tüysüz, H.; Salabas, E. L.; Weidenthaler, C.; Schüth, F. J. Am. Chem. Soc. 2008 130, 280.
(14) Kresge, C. T.; Leonowicz, M. E.; Roth, W. J.; Vartuli, J. C.; Beck, J. S. Nature 1992, 359, 710.
(15) Yanagisawa, T.; Shimizu, T.; Kuroda, K.; Kato, C. Bull. Chem. Soc. Jpn. 1990, 63, 988.
(16) Zhao, D.; Huo, Q.; Melosh, N.; Fredrickson, G. H.; Chmelka, B. F.; Stucky, G. D. Science 1998, 279, 548.
(17) Kleitz, F.; Choi, S. H.; Ryoo, R. Chem. Commun. 2003, 2136.
(18) Sinha, A. K.; Suzuki, K. Angew. Chem., Int. Ed. 2005, 44, 271.
(19) (a) Zhang, Z.; Hicks, R. W.; Pauly, T. R.; Pinnavaia, T. J. J. Am. Chem. Soc. 2002, 124, 1592. (b) Niesz, K.; Yang, P.; Somorjai, G. A. Chem. Commun. 2005, 1986. (c) Kuemmel, M.; Grosso, D.; Boissiere, C.; Smarsly, B.; Brezesinski, T.; Albouy, P. A.; Amenitsch, H.; Sanchez, C. Angew. Chem., Int. Ed. 2005, 44, 4589. (d) Yuan, Q.; Yin, A. X.; Luo, C.; Sun, L. D.; Zhang, Y. W.; Duan, W. T.; Liu, H. C.; Yan, C. H. J. Am. Chem. Soc. 2008, 130, 3465.
(20) Yang, P.; Zhao, D.; Margolese, D. I.; Chmelka, B. F.; Stucky, G. D. Nature 1998, 396, 152.
(21) Lyons, D. M.; Harman, L. P.; Morris, M. A. J. Mater. Chem. 2004, 14, 1976.
(22) Ryoo, R.; Joo, S. H.; Jun, S. J. Phys. Chem. B 1999, 103, 7743.
(23) Lu, A. H.; Schüth, F. Adv. Mater. 2006, 18, 1793.
(24) Tian, B. Z.; Lui, X.; Solovyov, L.; Liu, Z.; Yang, H.; Zhang, Z.; Xie, S.; Zhang, F.; Tu, B.; Yu, C.; Terasaki, O.; Zhao, D. J. Am. Chem. Soc. 2004, 126, 865.
(25) Wang, Y.; Yang, C. M.; Schmidt, W.; Spliethoff, B.; Bill, E.; Schüth, F. Adv. Mater. 2005, 17, 53.
(26) Tüysüz, H.; Lehmann, C. W.; Bongard, H.; Schmidt, R.; Tesche, B.; Schüth, F. J. Am. Chem. Soc. 2008, 130, 11510.
(27) Tian, B.; Lui, X.; Yang, H.; Xie, S.; Yu, C.; Tu, B.; Zhao, D. Adv. Mater. 2003, 15, 1370.
(28) Jiao, K.; Zhang, B.; Yue, B.; Ren, Y.; Liu, S.; Yan, S.; Dickinson, C.; Zhou, W.; He, H. Chem. Commun. 2005, 5618.
(29) Jiao, F.; Harrison, A.; Hill, A. H.; Bruce, P. G. Adv. Mater. 2007, 19, 4063.
(30) Jiao, F.; Harrison, A.; Jumas, J. C.; Chadwick, A. V.; Kockelmann, W.; Bruce, P. G. J. Am. Chem. Soc. 2006, 128, 5468.
(31) Jiao, F.; Jumas, J. C.; Womes, M.; Chadwick, A. V.; Harrison, A.; Bruce, P. G. J. Am. Chem. Soc. 2006, 128, 12905.
(32) Jiao, F.; Hill, A. H.; Harrison, A.; Berko, A.; Chadwick, A. V.; Bruce, P. G. J. Am. Chem. Soc. 2008, 130, 5262.
(33) Lu, A. H.; Schmidt, W.; Taguchi, A.; Spliethoff, B.; Tesche, B.; Schüth, F. Angew. Chem., Int. Ed. 2002, 41, 3489.
(34) Roggenbuck, J.; Tiemann, M. J. Am. Chem. Soc. 2005, 127, 1096.
(35) Dibandjo, P.; Bois, L.; Chassagneux, F.; Cornu, D.; Letoffe, J. M.; Toury, B.; Babonneau, F.; Miele, P. Adv. Mater. 2005, 17, 571.
(36) Liu, Q.; Wang, A. Q.; Wang, X. D.; Zhang, T. Chem. Mater. 2006, 22, 5155.
(37) Fang, Y.; Hu, H. J. Am. Chem. Soc. 2006, 128, 10636.
(38) Lai, X. Y.; Li, X. T.; Geng, W. C.; Tu, J. C.; Li, J. X.; Qiu, S. L. Angew. Chem., Int. Ed. 2007, 46, 738.
(39) Wagner, T.; Waitz, T.; Roggenbuck, J.; Froba, M.; Kohl, C. D.; Tiemann, M. Thin Solid Films 2007, 515, 8360.
(40) Skumryev, V.; Stoyanov, S.; Zhang, Y.; Hadjipanayis, G.; Givord, D.; Nogues, J. Nature 2003, 423, 850.
(41) An, K.; Lee, N.; Park, J.; Kim, S. C.; Hwang, Y.; Park, J. G.; Kim, Y. J.; Park, Y. H.; Han, M. J.; Yu, J.; Hyeon, T. J. Am. Chem. Soc. 2006, 128, 9753.
(42) Lagunas, A.; Payeras, A. M. I.; Jimeno, C.; Pericas, M. A. Chem. Commun. 2006, 1307.
(43) Zhang, Y.; Zhong, X.; Zhu, J.; Song, X. Nanotechnology 2007, 18, 195605.
(44) Toneguzzo, P.; Guillaume, V.; Acher, O.; Fievet-Vincent, F.; Fievet, F. Adv. Mater. 1998, 10, 1032.
(45) Feldman, C. Adv. Funct. Mater. 2003, 13, 101.
(46) Sinha, A.; Sharma, P. Mater. Res. Bull. 2002, 37, 407.

JA806202V